Journal of Organometallic Chemistry 775 (2015) 178–187

Contents lists available at ScienceDirect

Journal of Organometallic Chemistry

journal homepage: www.elsevier.com/locate/jorganchem

Pyridyl- and diphenylphosphinoethyl-functionalised *N*-heterocyclic carbene platinum methyl complexes

Nikolaos Tsoureas [a], Andreas A. Danopoulos [b, c, *]

[a] School of Life Sciences, University of Sussex, Sussex House, Falmer, Brighton, BN1 9RH, UK
[b] Institute for Advanced Study (USIAS), Université de Strasbourg, 67081 Strasbourg, France
[c] Laboratoire de Chimie de Coordination, Institut de Chimie UMR 5177, Université de Strasbourg, 4 rue Blaise Pascal, 67081 Strasbourg, France

ARTICLE INFO

Article history:
Received 17 February 2014
Received in revised form
9 July 2014
Accepted 10 July 2014
Available online 21 July 2014

Keywords:
N-Heterocyclic carbenes
Platinum
Cationic
Weakly coordinating
Alkyl complexes

ABSTRACT

The novel platinum (II) dimethyl complexes Pt(κ^2-L1)Me$_2$ and Pt(κ^2-L1)Me$_2$ (**1**), Pt(κ^2-L2a)Me$_2$ (**2a**) and Pt(κ^2-L2b)Me$_2$ (**2b**) bearing the functionalised *N*-heterocyclic carbenes (NHCs), **L1** = 1-(2-diphenylphosphinoethyl)-3-(2,6-di*iso*propyl-phenyl)-imidazol-2-ylidene, **L2a** = 1-(2-pyridyl)-3-(2,6-di*iso*propyl-phenyl)-imidazol-2-ylidene, **L2b** = 1-(2-(3-picolinyl))-3-(2, 6-di*iso*propyl-phenyl)-imidazol-2-ylidene, react with the acid [H(Et$_2$O)$_2^+$B(Ar^F)$_4^-$], Ar^F = 3, 5-(CF$_3$)$_2$C$_6$H$_3$, in the presence of various neutral donors (**Dn**) to give the salts [{Pt(κ^2-L)(Me)(Dn)}$^+${B(Ar^F)$_4$}$^-$], where **Dn** occupies specifically the site *trans* to the P and the C$_{NHC}$ donor atoms of the coordinated ligands **L1** and **L2a**, **L2b**, respectively. Spectroscopic data give evidence that the same selectivity prevails when other acids are employed. Activation of the Cl–CH$_2$Cl bond by **2b** led to [Pt(κ^2-L2b)(Me)Cl], while reaction of CH$_3$I with the dimethyl complexes led to isolable [Pt(κ^2-L)Me$_3$I] species.

Introduction

Platinum *N*-heterocyclic carbene (NHC) complexes of the type Pt(IMes)$_2$, IMes = 1,3-dimesitylimidazol-2-ylidene, were among the first reported transition metal complexes with NHC ligands after the introduction of stable imidazol-2-ylidenes [1]. Since then, the study of Pt complexes with monodentate NHCs continued, albeit at substantially slower pace than Pd complexes, mainly aiming at the development of novel catalysts for the hydrosilylation of alkenes and alkynes [2,3] and various types of C–H bond activation, including the C2–H of imidazoliums [4]. Recently, starting from [Pt(μ-Me$_2$S)Me$_2$]$_2$ and NHCs, NHC = IBu^t, IPr^i, IMes, diverse reactivity was observed, dependent on the steric properties of the NHCs, and led to either Pt(NHC)$_2$Me$_2$, coordinated NHC wingtip metallation *via* C–H activation, ethane reductive elimination, or abnormal NHC coordination [5]. The Pt(III) species [Pt(IPr)$_2$(I)$_2$]$^+$ obtained by the oxidation of [Pt(IPr)$_2$(Me)I] has been described [6]. Small monodentate NHCs with [Pt(IV)Me$_3$IL$_m$] or [Pt(IV)Me$_3$(Me$_2$CO)$_3$]BF$_4$, NHC = 1,3-dimethyl-imidazol-2-ylidene, 3-methyloxazol-2-ylidene, L = pyridine, *m* = 0, 2, led to diverse Pt(II) or Pt(IV) products, depending on the nature of the NHC used [7]. Chelating bidentate bis-NHC complexes of Pt(II)/(IV) have been studied in relation to Shilov-type C–H activation and alkane functionalisation and as possessing unique photophysical properties [8–11]. Furthermore, Pt complexes with bidentate ligands comprising NHCs functionalised with N-donors (pyridine, picoline, lutidine *etc.*) or cyclometallated, tridentate 'pincer' NHC ligands (aryl C$^-$-donor) have been studied for catalysis applications (hydroamination and hydrovinylation reactions) [12,13] and in relation to their interesting photophysical properties (luminescence, vapochromic behaviour *etc.*) [14,15], which can be combined with cytotoxicity for medicinal applications [16]. Oxidative addition and reductive elimination reactions involving Pt(II) and Pt(IV) methyl complexes stabilised by the linear κ^2- or κ^3-bis-1, 3-di(2-picolyl)imidazol-2-ylidene ligands have also been briefly studied [17].

We have described palladium dimethyl complexes with the chelating bidentate 2-diphenylphosphinoethyl-, 2-pyridyl- and 2-(3-picolyl)-functionalized NHCs (**L1** and **L2a**, **L2b**, respectively, see Scheme 1) and their protonolysis by [H(Et$_2$O)$_2$]$^+$[B(Ar^F)$_4$]$^-$ followed by association of a neutral donor (*e.g.* pyridine, MeCN *etc.*) at the created vacant site. The regiospecificity of the substitution, although in line with the relative *trans* influence of the pyridine and NHC donors of **L2a** and **L2b**, was unexpected for the P and NHC donors of the **L1**. Rationalisation of the observations by DFT methods invoked a subtle balance of electronic and steric factors and secondary

* Corresponding author. Institute for Advanced Study (USIAS), Université de Strasbourg, 67081 Strasbourg, France.
E-mail addresses: N.Tsoureas@sussex.ac.uk (N. Tsoureas), danopoulos@unistra.fr (A.A. Danopoulos).

http://dx.doi.org/10.1016/j.jorganchem.2014.07.010
0022-328X/

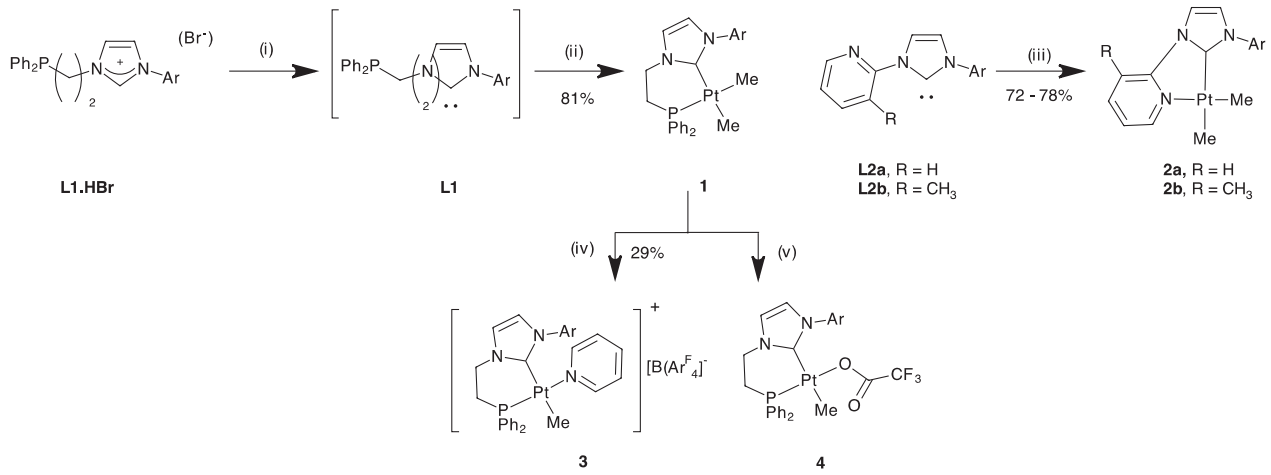

Scheme 1. The synthesis of Pt(II) dimethyl complexes, Ar = 2,6-$^{i}Pr_2C_6H_3$ (DiPP): (i) 1 equiv. $KN(SiMe_3)_2$, THF; (ii) $[Pt(\mu\text{-}Me_2S)Me_2]_2$, THF; (iii) $[Pt(\mu\text{-}Me_2S)Me_2]_2$, THF; (iv) 1 equiv. $[H(Et_2O)_2]^+[B(Ar^F)_4]^-$ in CH_2Cl_2 (−78 °C, −40 °C) followed by 1 equiv. pyridine (−40 °C); (v) 1 equiv. CF_3COOH in CD_2Cl_2, room temperature.

(agostic) interactions [18,19]. Protonolysis with CF_3COOH followed the same selectivity albeit association of CF_3COO^- with the Pd complex at the created vacant site was observed.

As an extension of these studies, herein we describe (i) novel Pt(II) dimethyl complexes coordinated by the ligands κ^2-**L1** and κ^2-**L2a** or κ^2-**L2b** ligand coordination, and (ii) a range of novel cationic derivatives obtained either by their protonolysis with $[H(Et_2O)_2]^+[B(Ar^F)_4]^-$ in the presence of neutral donors (**Dn**), or by acids with coordinating anions. We also report the reactions of Pt(II) dimethyl complexes with MeI leading to stable Pt(IV) species. The synthetic transformations are summarised in Schemes 1–3.

Results and discussion

Neutral Pt dimethyl complexes

The synthesis of the neutral Pt dimethyl complexes involved the substitution of the labile ligand Me_2S in $[Pt(\mu\text{-}Me_2S)(CH_3)_2]_2$ either by the *in situ* generated NHC (for **L1**) or the isolated free NHC (for **L2a** and **L2b**) (Scheme 1). The new complexes were isolated in high yields as colourless or yellow, air stable powders. Solutions of **1** and **2a**, **2b** in CH_2Cl_2 have limited stability even under inert atmosphere (*i.e.* after 2–3 h the formation of a mixture of species becomes evident by ^{1}H NMR, see also below). However, characterisation of the complexes was carried out by analytical, spectroscopic (taking care to minimise the duration of the experiment) and diffraction methods.

The ^{1}H NMR spectra of the complexes concur with non-symmetric solution structures. Thus the inequivalent Pt–CH_3 signals appeared as a pair of doublets or as a pair of singlets for **1** or **2a**, **2b**, respectively, accompanied by Pt satellites. The Pt–CH_3 signals in **1** are shifted upfield relative to the corresponding signals in **2a** and **2b**. The shielding may be ascribed to the better σ-donor ability of phosphine donor in **1**; interestingly, the value of the $^2J_{Pt-H}$ of the Pt–CH_3 signals is larger in **2a**, **2b** than the in **1**. The stronger electron donating character of the **L1** may also be responsible for the

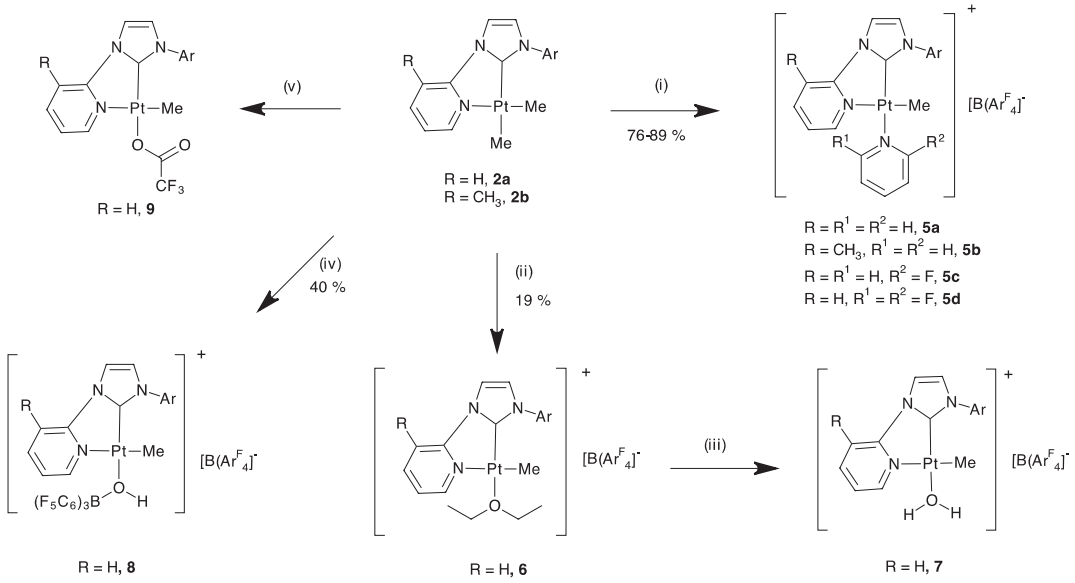

Scheme 2. The synthesis of Pt methyl complexes containing the ligands **L2a** and **L2b**: (i) 1 equiv. $[H(Et_2O)_2]^+[B(Ar^F)_4]^-$ in CH_2Cl_2 (−78 °C, −40 °C) followed by 1 equiv. pyridine derivative (−40 °C) (76–89%); (ii) 1 equiv. $[H(Et_2O)_2]^+[B(Ar^F)_4]^-$ and 1 equiv. CF_3CH_2OH in CH_2Cl_2 (−78 °C, room temperature) followed by crystallisation from ether (19%); (iii) H_2O in chlorobenzene-d^5; (iv) $B(C_6F_5)_3$, H_2O, ether, (−78 °C to room temperature, 40%); (v) 1 equiv. CF_3COOH, CD_2Cl_2, room temperature.

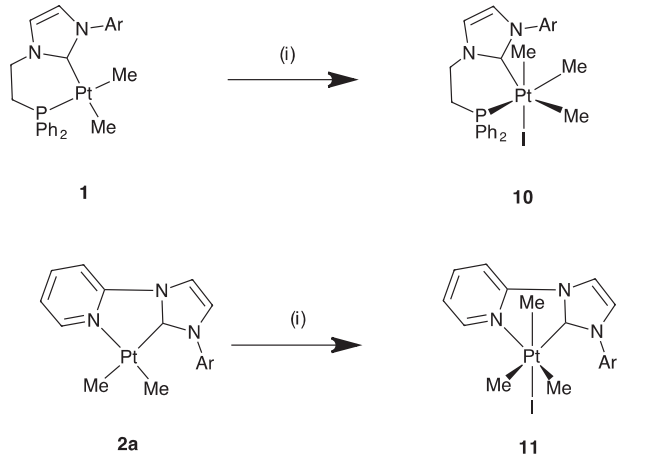

Scheme 3. Reactions of the platinum dimethyl complexes with MeI: (i) 1 equiv. MeI, CH_2Cl_2, room temperature.

upfield shift in the $^{195}Pt\{^1H\}$ NMR spectra of **1** (δ −4257.9, d, $^1J_{Pt-P}$ = 1822.5 Hz) compared to **2a** and **2b** (δ −3764.1 and δ −3763.9, both s), respectively.

The position of the inequivalent Pt–CH_3 relative to the *trans* donors in the complexes **2a** and **2b** was determined by NOESY NMR spectroscopy: the downfield signals (0.44 and 0.45 ppm) were assignable to methyl groups situated *trans* to the NHC moiety. The coordinated phosphine in **1** appears at δ 12.4 ($^1J_{Pt-P}$ = 1822.5 Hz). Surprisingly, and in contrast to **2a** and **2b**, the Pt–CH_3 and Pt–C_{NHC} in the $^{13}C\{^1H\}$ NMR spectrum of **1** could not be observed.

The structures of **1** and **2a** were confirmed crystallographically (Figs. 1 and 2, respectively).

In both cases the coordination geometry at Pt is square planar, with the donor atoms of the ligands **L1** and **L2a** occupying two *cis* positions. In **1** the two Pt–CH_3 bond distances, (2.075(4) and 2.085(4) Å), are equal within the observed esds, a trend also observed in the analogous Pd complex reported previously [19]. Thus, there is no significant difference in the *trans* influence of the phosphine and the NHC donors. However, the Pt–C_{NHC} bond is slightly shorter than the σ-donating Pt–CH_3; interestingly, the Pt–C_{NHC} *is significantly shorter* than the corresponding bond in the Pd analogue.

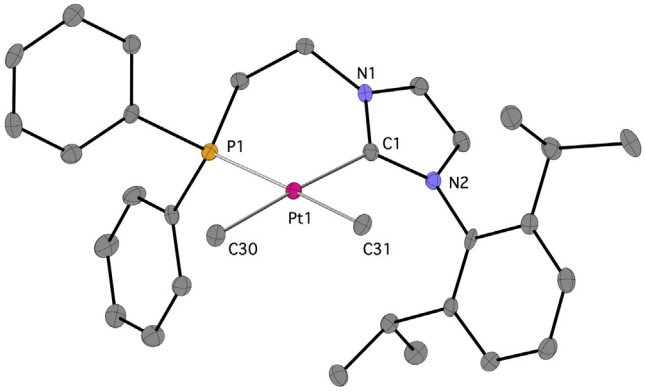

Fig. 1. The structure of **1**; ellipsoids are at the 40% probability level. Selected distances (Å) and angles (°): C1–Pt1 = 2.031(5), Pt1–C30 = 2.075(5), C31–Pt1 = 2.085(4), Pt1–P1 = 2.249(1), C1–N1 = 1.348(5), N2–C1 = 1.369(6), C1–Pt1–C31 = 95.2(2), C31–Pt1–C30 = 84.6(2), C30–Pt1–P1 = 89.5(1), P1–Pt1–C1 = 90.9(1), N2–C1–N1 = 102.7(3).

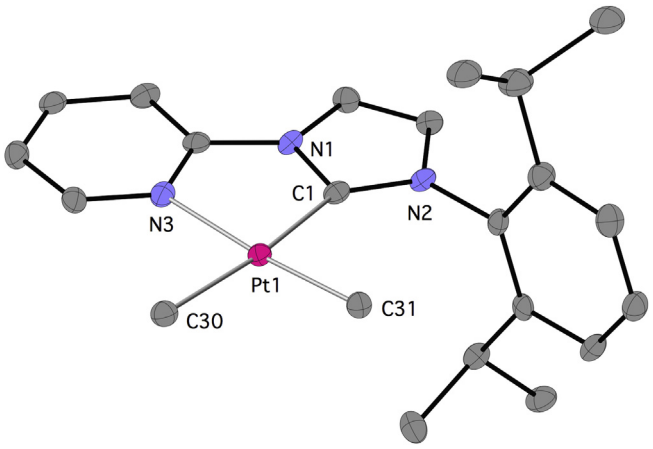

Fig. 2. The structure of **2a**; ellipsoids are at the 30% probability level. Only one position of a disordered *o*-^{i}Pr is shown. Selected distances (Å) and angles (°): Pt1–C30 = 2.087(5), Pt1–C31 = 2.044(5), Pt1–N3 = 2.128(5), Pt1–C1 = 2.006(5), N1–C1 = 1.381(7), C1–N2 = 1.355(7), N3–Pt1–C1 = 78.2(2), C30–Pt1–N3 = 93.7(2), C31–Pt1–C1 = 98.0(2), C30–Pt1–C31 = 90.1(2), N1–C1–N2 = 103.0(4).

In **2a** the two Pt–CH_3 bonds exhibit significantly different bond distances: 2.087(6) Å (*trans* to C_{NHC}) and 2.044(5) Å (*trans* to N_{py}), in line with the different *trans* influences of the corresponding donors. The Pt–C_{NHC} bond distances are virtually the same in **1** and **2a**. In **2a** the NHC plane slightly deviates from the coordination plane, defined by the Pt and the two methyl groups, and the plane defined by the pyridine ring by 5.44° and 2.97°, respectively.

As mentioned previously, all three platinum dimethyl complexes have limited stability in chlorinated solvents. Attempts to crystallise **2b** from CH_2Cl_2/ether gave crystals of the complex **2b**Cl the identity of which was established crystallographically (see Fig. 3). The crystals were insoluble in all inert organic solvents, which hampered spectroscopic characterisation.

It is clearly evident that the CH_3 that was *trans* to the NHC in **2b** was replaced by one Cl atom originating from the CH_2Cl_2 solvent. The Pt–C_{NHC}, Pt–N_{py} and Pt–CH_3 bond distances are equal to the

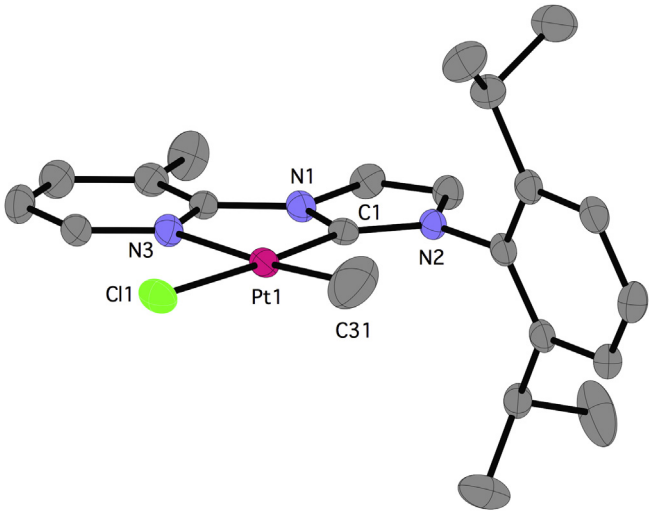

Fig. 3. The structure of **2b**Cl from the reaction of **2b** with CH_2Cl_2; ellipsoids are at 40% probability level. Only one position of a disordered *o*-^{i}Pr is shown. Selected distances (Å) and angles (°): N3–Pt1 = 2.112(5), C1–Pt1 = 1.935(5), Pt1–C31 = 2.04(1), Pt1–Cl1 = 2.335(2), N1–C1 = 1.374(8), C1–N2 = 1.333(7), N3–Pt1–C1 = 78.3(2), C1–Pt1–C31 = 103.5(4), C31–Pt1–Cl1 = 81.5(4), Cl1–Pt1–N3 = 96.7(1), N1–C1–N2 = 105.5(5).

corresponding ones in **2a**. A plausible mechanism for the formation of the chlorinated product may involve oxidative addition of the Cl–CH_2Cl bond, followed by reductive elimination of chloroethane. Attempts to substitute one methyl of **2a** or **2b** with Cl by reaction with HCl (2 M solution in ether) in CH_2Cl_2 led to decomposition products. Interestingly, the oxidative addition of CH_2Cl_2 has also been observed with the corresponding palladium dimethyl complex [19]; in either case the chloride was introduced at the site *trans* to the NHC donor. It appears that the increased lability aptitude of the Pt–CH_3 *trans* to the NHC originates from the weaker Pt–C_{Me} bond and is a common feature of both the Pd and Pt complexes with ligands **L2a** and **L2b** (see also below) and contrasts the behaviour of the complexes with the ligand **L1**, where the Pt–C_{Me} bond *trans* to the PPh_2 functionality is preferentially cleaved.

Cationic Pt complexes

Organometallic cations are ubiquitous in homogeneous catalysis, for example in reactions leading to C–Y bond formation, Y = H, C, Si, polymerizations and C–H activation processes [20–23]. In the latter process Pt complexes have been commonly employed as catalysts. The currently studied systems use as cation precursors symmetrical chelating N-donor (bipyridine, diimine) and P-donor (diphosphine) Pt(II) dialkyls. Crucially, the generation of the reactive cationic complex species required the use of acids with weakly coordinating anions and weakly coordinating solvents, in order to minimise competition with the C–H bond of the substrate to be activated for a metal coordination site.

In the following, we describe cationic Pt(II) complexes obtained by protonolysis of the dimethyl complexes **1** and **2a**, **2b** in the presence of the donor **Dn**. The attack of the electrophilic H^+ is conceivable either at the metal, giving formally Pt(IV) cations, which can reductively eliminate CH_4 to Pt(II) cations and associate **Dn**; alternatively, direct electrophilic attack of H^+ on the coordinated CH_3 in the presence of **Dn** can lead to the same species (see Scheme 4).

In all cases studied the preferentially abstracted Me group is *trans* to the P donor (in the protonolysis with **1**) or *trans* to the NHC (in the protonolysis with **2a**). These observations are in agreement with observations in analogous Pd complexes [18,19].

Monitoring the reaction of **1** with $[H(Et_2O)_2]^+[B(Ar^F)_4]^-$ (1 equiv.) and pyridine in CD_2Cl_2 by ^1H NMR spectroscopy, showed the formation of two species in *ca.* 2:1 ratio. The Pt–CH_3 region contained two distinct CH_3 signals; four different signals assignable to $CHMe_2$ of the DiPP (2:2:1:1 ratio) were also seen. Other spectral features were also doubled in 2:1 ratio. The $^{31}P\{^1H\}$ consisted of one signal at 10.1 ppm ($^1J_{Pt-P}$ = 746.0 Hz), and one at 8.7 ppm ($^1J_{Pt-P}$ = 1977.1 Hz). Repeating the reaction in ether followed by work-up which included layering of the ether with pentane, afforded crystals. An X-ray diffraction study revealed that the crystals corresponded to the formation of **3** (Scheme 1), where electrophilic attack and pyridine coordination has taken place at the site *trans* to the phosphine moiety of the bidentate ligand. Unfortunately, the quality of the data was not sufficient to produce a publishable model. Elemental analytical data of the crystalline material supported the proposed crystallographic model. Surprisingly, the NMR data obtained after redissolving the crystals in CD_2Cl_2 were identical to those described above, implying the reformation of two species. A proposal to rationalise these observations may involve association of CD_2Cl_2 with **3** or reversible oxidative addition/reductive elimination of CD_2Cl_2. Adducts of CH_2Cl_2 with cationic Pt(II) complexes are rare but known [24] and the role of oxidative addition of CH_2Cl_2 to Pt(II) methyl complexes has been discussed [25]. Reversible oxidative addition of MeI to 2,6-(bis-carbene)-pyridine 'pincer Pt complexes has been described briefly [12]. Attempts to detect platinum species in solution by mass spectrometry or study the postulated equilibrium by variable temperature ^1H NMR spectroscopy were inconclusive.

The reaction of **1** with trifluoroacetic acid (1 equiv.) resulted in the cleavage of one of the Pt–Me bonds and the formation of the product formulated as **4** (Scheme 1). This was evidenced by the disappearance of one Pt–CH_3 signal in the ^1H NMR spectrum of **1** after the addition of the acid. The protons of the remaining Pt–CH_3 ligand resonate at 0.08 ppm ($^2J_{Pt-H}$ = 35.5 Hz)); furthermore the signal in the $^{31}P\{^1H\}$ NMR spectrum of **4** revealed a downfield shift after CH_3 abstraction (δ 11.7 ppm in **1** and δ 19.6 ($^1J_{Pt-P}$ = 2017.8 Hz) in **4**.

The reaction of **2a** and **2b** with $[H(Et_2O)_2]^+[B(Ar^F)_4]^-$ in the presence of a neutral donor **Dn** led to the isolation of complexes **5a**–**d** (Scheme 2). Their formation was confirmed by ^1H and ^{13}C NMR spectroscopy. Of high diagnostic value was the replacement of the two Pt–Me signals of **2a** and **2b** by one downfield shifted, corresponding to the single Pt–Me of the cations in **5a**–**d**. The presence of only one Pt–Me signal in the ^1H, ^{13}C and ^{195}Pt NMR spectra supported the regioselectivity of the abstraction/substitution sequence. The diastereotopic methyl groups of the DiPP wingtip appear as two doublets, even when **Dn** is nonsymmetric (*i.e.* the 2-fluoro-pyridine in **5c**), which implies rapid rotation at the Pt–Dn bond. The proposed geometries of the cationic complexes were confirmed by NOESY spectroscopy. In the ^{19}F spectra of **5a**–**d** the noncoordinating anion appears as singlet, while in **5c** and **5d** additional singlets due to fluoro-pyridines are observed; in **5d** it is accompanied by Pt satellites (J_{Pt-F} = 110.2 Hz), implying a long range interaction of the *o*-F-substituents with Pt.

The structures of **5b** and **5c** were determined crystallographically and are shown in Figs. 4 and 5.

The geometry around the metal centres is virtually square planar with the ligand **L2b** occupying two *cis* positions, forming a bite angle of 78.11(12)°. The pyridine **Dn** is situated *trans* to the NHC and the plane of the heterocycle is perpendicular to the coordination plane (88.97°). The NHC and the tethered pyridine planes form an angle of 17.18°. In **5c** the 2-fluoro-pyridine is disordered over two positions, one with the fluorine atom above the coordination plane and the other below. This is in agreement with the NMR data discussed above.

Monitoring of the protonolysis of **2a** with $[H(Et_2O)_2]^+[B(Ar^F)_4]^-$ in CH_2Cl_2 using styrene as **Dn** showed broad and uninterpretable NMR spectra, however, after evaporation of the volatiles under reduced pressure and crystallisation of the residue from ether/pentane gave sensitive crystals of **6** in low yields. The identity of **6** was established crystallographically (see Fig. 6).

The cation in **6** comprises a square planar Pt in which the coordination site *trans* to the NHC donor of the ligand **L2a** is now occupied by an ether molecule. The Pt–C_{NHC}, Pt–Me and Pt–N

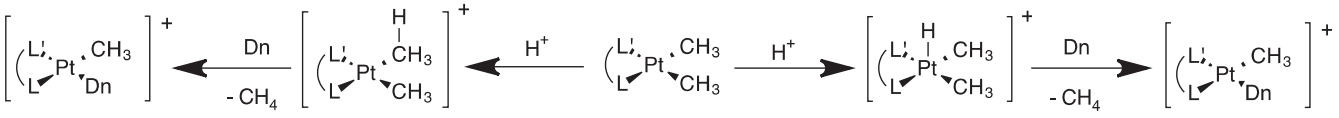

Scheme 4. Alternative sites of electrophilic attack (Pt, coordinated CH_3) leading to cationic complexes stabilized by the donor **Dn**.

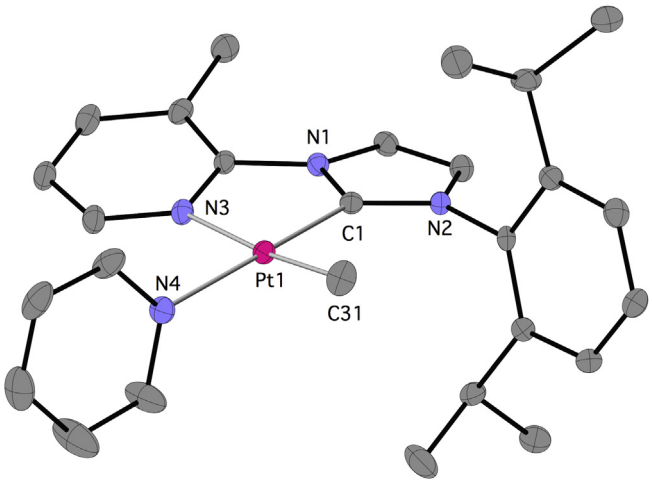

Fig. 4. The structure of the cation in **5b**. Selected distances (Å) and angles (°): Pt1–C31 = 2.050(5), N4–Pt1 = 2.068(2), Pt1–N3 = 2.130(3), C1–Pt1 = 1.945(2), N2–C1 = 1.349(4), C1–N1 = 1.375(5), C1–Pt1–N3 = 78.1(1), C31–Pt1–C1 = 101.4(2), N4–Pt1–C31 = 85.3(1), N4–Pt1–N3 = 95.6(1), N2–C1–N1 = 104.2(3).

bond distances are equal within esds with the ones found in the cations of **5b** and **5c**. Structurally characterised Pt(II)-ether cations complexes are very rare and sometimes unstable in solution at room temperature [24,26,27]. Pt(II)-THF complexes are also very rare [28,29]. The structure of **6** in solution was studied by ^{1}H NMR spectroscopy after dissolving the crystals in commercial (not pre-dried) d^{5}-C_6H_5Cl; the presence of two ether molecules (1:1 ratio), corresponding to one coordinated and one crystallisation ether. In the spectrum, two singlets in 1:1 ratio were also observed at δ 1.5 and 1.9, the latter accompanied by platinum satellites ($^{2}J_{Pt-H}$ = 37.9 Hz); they were assigned to H_2O in C_6D_5Cl and H_2O coordinated after exchange with ether, respectively, leading to the formation of **7** (Scheme 2). When the NMR sample was shaken with one drop of D_2O, the ratio of coordinated to uncoordinated H_2O changed to 3:1, while the ratio of coordinated to uncoordinated ether changed to 1:8. The sample was heated to 45 °C for 10 min upon which time the coordinated/uncoordinated H_2O ratio increased to 4:1, while the two ether resonances collapsed into one

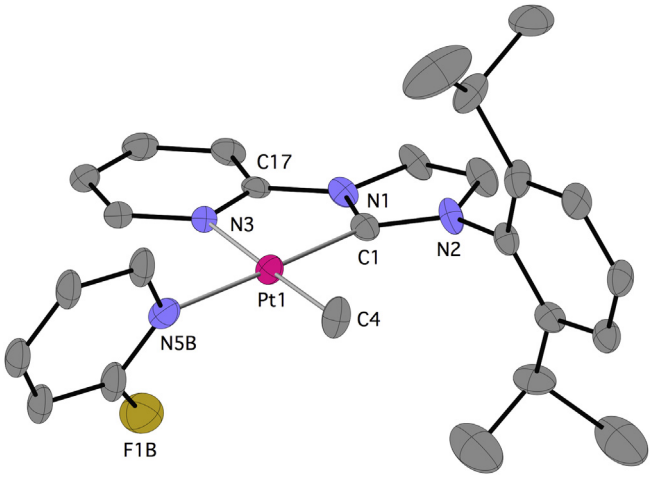

Fig. 5. The structure of the cation in **5c**. Selected distances (Å) and angles (°): Only one disordered 2-fluoro-pyridine ligand is shown. Pt1–C1 = 1.938(7), Pt1–N3 = 2.131(6), Pt1–C4 = 2.053(8), Pt1–N5B = 2.05(1), N1–C1 = 1.38(1), C1–N2 = 1.351(8), C1–Pt1–C4 = 99.3(3), C1–Pt1–N3 = 78.8(3), N3–Pt1–N5B = 98.3(5), N5B–Pt1–C4 = 83.6(5), N2–C1–N1 = 103.7(6).

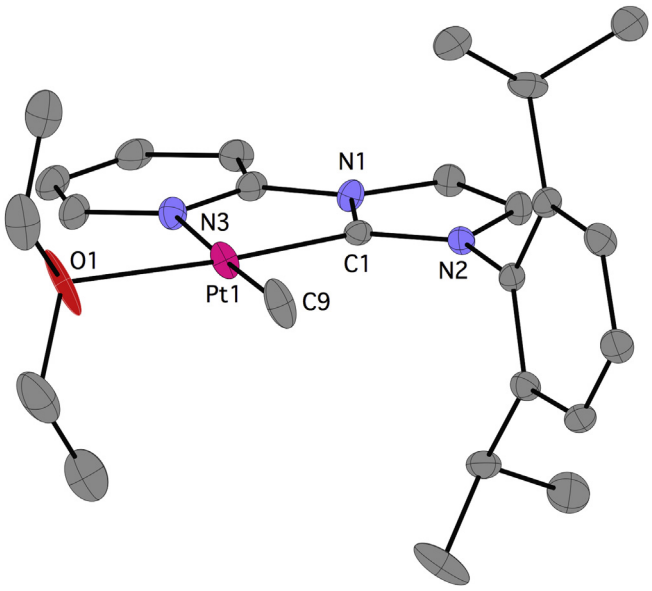

Fig. 6. The structure of the cation in **6**. Selected distances (Å) and angles (°): N3–Pt1 = 2.126(5), Pt1–C1 = 1.937(4), Pt1–C9 = 2.048(8), Pt1–O1 = 2.180(4), N2–C1 = 1.337(6), C1–N1 = 1.368(7), N3–Pt1–C1 = 79.4(2), C9–Pt1–C1 = 98.6(2), N1–C1–N2 = 104.9(4), O1–Pt1–N3 = 90.7(2), O1–Pt1–C9 = 91.2(2).

quartet at 3.4 ppm, indicating that the equilibrium was shifted towards the H_2O coordinated cationic species **7**. The Pt–*Me* protons in **6** appear at 0.22 ppm ($^{2}J_{Pt-H}$ = 35.1 Hz). This signal is shifted upfield compared to complexes [Pt($R_2PCH_2CH_2PR_2$)(CH_3)(OEt_2)] BAr^{F}_4] (R = Et, Cy) [30]. Unlike the bisphosphine monocationic complexes, **6** is stable in the presence of water, and no (μ-OH) decomposition complexes were observed.

The reaction of **2a** with one equiv. of $B(C_6F_5)_3$ in the presence of H_2O was undertaken in the absence of a donor ligand (Scheme 2). This combination is known to provide $[H]^+[(B(C_6F_5)_3(OH)]^-$ [31], which has been used as acid on many occasions, including platinum chemistry [32]. The identity of **8** was established from its ^{1}H NMR spectrum, in which one peak at −0.01 ppm (Pt satellites with $^{2}J_{Pt-H}$ = 37.7 Hz) was assigned to Pt–*Me* and a broad singlet at 2.93 ppm to OH. The location of the Pt–Me bond relative to the donors of ligand **L2a** was confirmed by NOESY experiments which revealed that the Pt–Me bond that was *trans* to the NHC was preferentially cleaved by the acid.

The structure of **8** was unambiguously established crystallographically (Fig. 7).

The geometry around Pt is square planar with the coordination sphere comprising the chelating **L2a**, one CH_3 and the $[B(OH)(C_6F_5)_3]^-$. The Pt–CH_3, Pt–C_{NHC} and Pt–$N_{pyridine}$ bond distances compare to those in **5b** and **5c**. The Pt–O bond distance (2.106(9) Å) in **8** is also the same within esds with the Pt–N(2-fluoropyridine) distance (2.095(7) Å) in **5c**. This is an indication that the $[B(OH)(C_6F_5)_3)]^-$ anion is not binding very strongly to Pt, possibly due to the electron withdrawing pentafluorophenyl groups.

Oxidative addition of MeI

The oxidative addition of MeI in the complexes **1** and **2a** was investigated (Scheme 3). In both cases the reaction takes place within seconds at room temperatures affording the Pt(IV) complexes **10** and **11**, respectively, in good yields. The formation of **10** and **11** was established by spectroscopic methods. Their ^{1}H NMR spectra confirmed the formation of non-symmetric structures. The

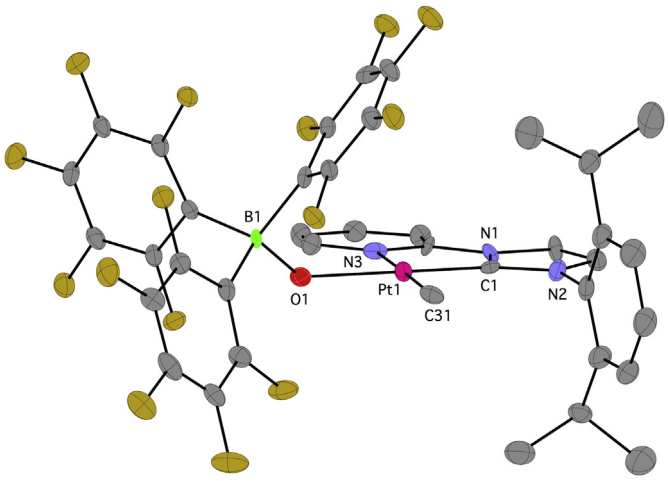

Fig. 7. The structure of **8**. Selected distances (Å) and angles (°): C1–Pt1 = 1.89(1), Pt1–N3 = 2.13(1), Pt1–C31 = 1.99(1), O1–Pt1 = 2.105(8), N2–C1 = 1.35(1), C1–N1 = 1.40(2), C1–Pt1–N3 = 80.3(5), C31–Pt1–C1 = 98.3(6), O1–Pt1–C31 = 90.6(5), O1–Pt1–N3 = 90.8(4), N2–C1–N1 = 100(1).

two characteristic doublets of the diastereotopic *o*-CH*Me*$_2$ of the DiPP wingtip in **1** and **2a**, were split into four distinct doublets in **10** and **11**. Furthermore, two *o*-*CH*Me$_2$ septets were observed in their ^{1}H NMR spectra. The Pt–C*H*$_3$ in the Pt(IV) products were shifted further downfield compared to the Pt(II) parent complexes. The Pt–C*H*$_3$ resonances in **10** and **11** were isochronous to related complexes of the type *fac*-[(PP)PtMe$_3$X] (X = I, OTf, PP = chelating phosphine) [33]. The ^{31}P{^{1}H} NMR signal in **10** was shifted upfield compared **1**. This trend has been observed during the oxidative addition of MeI and MeOTf to the Pt(II) complex [(dppe)PtMe$_2$] (dppe = diphenylphosphinoethane) [34].

The structure of **11** was determined crystallographically and is shown in Fig. 8.

The geometry around the Pt is octahedral with *fac*-arrangement of the methyl ligands. All Pt–Me distances are the same within the measured esds and comparable to the lengths of the Pt(II) complex **2a**. On the other hand the Pt–C$_{NHC}$ and Pt–N$_{pyridine}$ are longer in **11**.

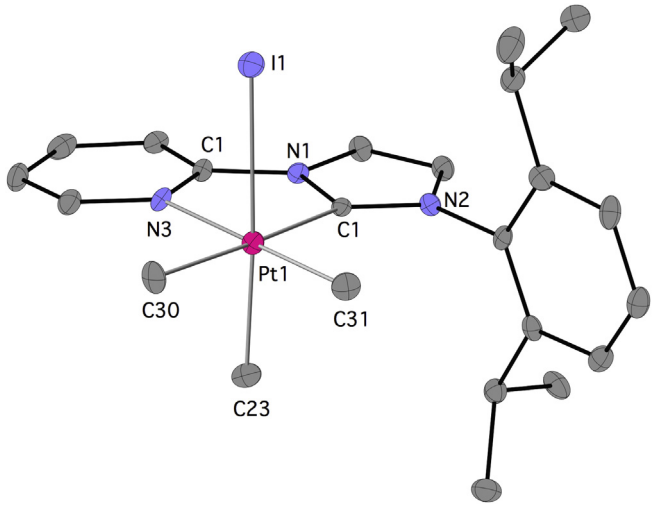

Fig. 8. The structure of **11**. Selected distances (Å) and angles (°): N3–Pt1 = 2.178(4), C1–Pt1 = 2.078(4), I1–Pt1 = 2.7902(4), Pt1–C31 = 2.060(5), Pt1–C30 = 2.089(4), N1–C1 = 1.378(6), N2–C1 = 1.342(5), N3–Pt1–I1 = 88.2(1), N3–Pt1–C30 = 97.5(2), C30–Pt1–C31 = 85.9(2), C31–Pt1–C1 = 99.5(2), N3–Pt1–C1 = 77.1(2), N3–Pt1–C23 = 89.5(2), N2–C1–N1 = 104.2(4).

On heating **11** in toluene-d^8 (40 °C, 80 °C 48 h) did not result in any reaction. Heating at 125 °C for 4 h resulted in extended decomposition as evidenced by the formation of black aggregates and minor peaks assignable to ethane (δ 0.83), C–H(imidazolium) (δ 10.5) and CH$_3$I (δ 2.16).

Conclusions

Neutral, square planar Pt(II) dimethyl complexes stabilised by the chelating bidentate diphenylphosphinoethyl- and 2-pyridyl-functionalised imidazol-2-ylidenes undergo selective protonolysis of the more reactive methyl group that is *trans*- to the P- or C$_{NHC}$-donors, respectively. The selectivity is the same to the previously observed in analogous Pd complexes and may be controlled by the electronic factors and weaker intramolecular agostic interactions. However, the reactivity of the Pt complexes is lower than the Pd analogues as can be established by the inertness of the former towards the weakly acidic (CF$_3$)$_2$CHOH and C$_6$F$_5$OH [19]. In dichloromethane the Pt(II)-dimethyl complexes exchange their more reactive methyl (same as in the protonolysis reactions) with chloride. The mechanism of the exchange may involve oxidative addition and reductive elimination from transient Pt(IV)Me(CH$_2$Cl)Cl species. However, oxidative addition of MeI gave isolable Pt(IV)Me$_3$I which on thermolysis failed to give ethane cleanly. The catalytic and photophysical properties of the novel Pt complexes are under further study.

Experimental

Elemental analyses were carried out by the microanalytical laboratory of London Metropolitan University. All manipulations involving organometallics were performed under nitrogen or argon in a Braun glove-box or using standard Schlenk techniques unless specified otherwise. Solvents were dried using standard methods and distilled under nitrogen prior use or passed through columns of activated alumina and subsequently purged with nitrogen or argon.

[Pt(μ-Me$_2$S)Me$_2$]$_2$ [35] the salt **L1**·HBr [18,19] and the NHCs compounds **L2a** and **L2b** [36,37] were prepared according to literature procedure. The acid [H(Et$_2$O)$_2$]$^+$[B(Ar^F)$_4$]$^-$ was prepared by modification of the literature procedure [38] using a 2 M HCl solution in ether instead of gaseous HCl for its generation. Iodomethane, dimethylsulfide, trifluoroacetic acid, 2-fluoropyridine, tris(pentafluorophenyl)borane and all other starting materials were from Aldrich and were used as received.

cis-Pt(κ^2-L1)(CH$_3$)$_2$ **1**

To a solution of 0.080 g (0.14 mmol) of [Pt(μ-Me$_2$S)Me$_2$]$_2$ in THF at −78 °C was added a solution of the free carbene **L1**, generated from 0.146 g (0.28 mmol) of imidazolium salt **L1**·HBr and 0.062 g of KN(SiMe$_3$)$_2$ (1.1 equiv. relative to the imidazolium salt) in THF (50 ml) at −50 °C. The reaction mixture was allowed to reach room temperature and stirred for 2 h. Removal of the volatiles under reduced pressure, extraction of the residue with CH$_2$Cl$_2$ (15 ml), filtration through Celite, evaporation of the volatiles under reduced pressure, washing of the residue with ether (10 ml) and pentane (2 × 10 ml), and drying under vacuum gave **1** as an off-white solid. The product decomposes after exposure to CHCl$_3$, prolonged exposure to CH$_2$Cl$_2$; is soluble in chlorobenzene or THF. Yield: 0.150 g (81%). Crystals of **1** were grown by layering a THF solution with pentane. ^{1}H NMR (CD$_2$Cl$_2$), δ: −0.18 (3H, d, $^3J_{P-H}$ = 7.7 Hz, Pt–C*H*$_3$, satellites appear as dd with $^3J_{P-H}$ = 7.7 Hz and $^2J_{Pt-H}$ = 29.0 Hz), −0.03 (3H, d, $^3J_{P-H}$ = 7.7 Hz, Pt–C*H*$_3$, satellites appear as dd with $^3J_{P-H}$ = 7.7 Hz and $^2J_{Pt-H}$ = 29.0 Hz), 0.93 (6H, d, $^3J_{H-H}$ = 6.9 Hz, CH(C*H*$_3$)$_2$), 1.14 (6H, d, $^3J_{H-H}$ = 6.9 Hz, CH(C*H*$_3$)$_2$),

2.30 (2H, m, [PPh$_2$C*H$_2$*CH$_2$-ylidene]PtMe$_2$), 2.82 (2H, sept., $^3J_{H-H}$ = 6.9 Hz, C*H*(CH$_3$)$_2$), 4.21 and 4.27 (1H each, m, [PPh$_2$CH$_2$C*H$_2$*-ylidene]PtMe$_2$), 6.76 (1H, m, aromatic), 7.01 (1H, m, aromatic), 7.15 (2H, distorted d, aromatic), 7.37 (7H, m, aromatic), 7.64 (4H, m, aromatic); ^{13}C{^{1}H} NMR (CD_2Cl_2), δ: no Pt–CH$_3$ resonances observed, 21.8 (s, CH(*C*H$_3$)$_2$), 24.4 (s, CH(*C*H$_3$)$_2$), 26.9 (d, $^1J_{P-C}$ = 14.2 Hz, [PPh$_2$*C*H$_2$CH$_2$-ylidene]PtMe$_2$), 27.5 (s, *C*H(CH$_3$)$_2$), 48.4 (d, $^2J_{P-C}$ = 10.4 Hz, [PPh$_2$CH$_2$*C*H$_2$-ylidene]PtMe$_2$), 118.6 (s, aromatic), 122.6 (s, aromatic), 122.9 (s, aromatic), 127.2 (d, J_{P-C} = 3.1 Hz, aromatic), 128.1 (s, aromatic), 128.8 (s, aromatic), 132.3 (d, J_{P-C} = 5.0 Hz, aromatic), 132.9 (d, $^1J_{P-C}$ = 11.4 Hz, aromatic), 136.1 (s, aromatic), 145.0 (s, aromatic); ^{31}P{^{1}H}-NMR (CD_2Cl_2), δ: 11.7 (s, [*P*Ph$_2$CH$_2$CH$_2$-ylidene]PtMe$_2$, $^1J_{Pt-P}$ = 1822.5 Hz); ^{195}Pt{^{1}H} NMR (CD_2Cl_2), δ: −4257.9 (d, $^1J_{Pt-P}$ = 1822.5 Hz, [PPh$_2$CH$_2$CH$_2$-ylidene]*Pt*Me$_2$); Anal. Found: C, 55.49; H, 5.79; N, 4.21%. Calcd for $C_{31}H_{39}N_2PPt$: C, 55.93; H, 5.90; N, 4.21%.

cis-Pt(κ^2-L2a)(CH$_3$)$_2$ ***2a***

A pre-cooled (−78 °C) solution of the free carbene **L2a** (0.085 g, 0.28 mmol) in THF was added by cannula to a cold (−78 °C) solution of 0.080 g (0.14 mmol) of [Pt(μ-Me$_2$S)Me$_2$]$_2$. After warming to room temperature the reaction mixture was stirred for 2 h and the volatiles were removed under reduced pressure to give a bright yellow solid residue, which was washed with ether and dried under vacuum. Yield: 0.115 g, (78%). ^{1}H NMR (CD_2Cl_2), δ: 0.29 (3H, s, Pt–C*H*$_3$, $^2J_{Pt-H}$ = 46.6 Hz), 0.45 (3H, s, $^2J_{Pt-H}$ = 31.2 Hz), 1.09 (6H, d, $^3J_{H-H}$ = 6.9 Hz, CH(C*H*$_3$)$_2$), 1.34 (6H, d, $^3J_{H-H}$ = 6.9 Hz, CH(C*H*$_3$)$_2$), 2.75 (2H, sept., $^3J_{H-H}$ = 6.9 Hz, C*H*(CH$_3$)$_2$), 6.58 (1H, d, $^3J_{H-H}$ = 2.0 Hz), 7.28 (3H, m, aromatic), 7.45 (2H, t, $^3J_{H-H}$ = 7.9 Hz, aromatic pyridine), 7.63 (1H, d, $^3J_{H-H}$ = 2.0 Hz, ylidene backbone), 8.09 (1H, ddt, J_{H-H} = 0.7 Hz, 1.5 Hz, 7.4 Hz Hz, aromatic pyridine), 9.07 (1H, s, m, aromatic pyridine); ^{13}C{^{1}H} NMR (CD_2Cl_2), δ: −31.4 (s, Pt–CH$_3$, $^1J_{Pt-C}$ = 401.9 Hz), −21.8 (s, Pt–CH$_3$, $^1J_{Pt-C}$ = 397.8 Hz), 22.2 (s, *C*H(CH$_3$)$_2$), 23.4 (s, CH(*C*H$_3$)$_2$), 27.6 (s, *C*H(CH$_3$)$_2$), 109.4 (s, ylidene backbone), 113.5 (s, ylidene backbone), 121.8 (s, aromatic), 122.9 (s, aromatic), 124.1 (s, aromatic), 129.1 (s, aromatic), 134.9 (s, aromatic), 137.7 (s, aromatic), 144.9 (s, aromatic), 146.2 (s, aromatic), 152.6 (s, aromatic), 189.5 (s, N*C*N, $^1J_{Pt-C}$ = 441.9 Hz); ^{195}Pt{^{1}H}–NMR(D$_2$O), δ: −3764.1. Found: C, 50.45; H, 5.38; N, 7.93%. Calcd for $C_{22}H_{29}N_3Pt$: C, 49.80; H, 5.51; N, 7.92%. Crystals were grown by slow diffusion of Et$_2$O into a CH_2Cl_2 solution of **2a**.

cis-Pt(κ^2-L2b)(CH$_3$)$_2$ ***2b***

This was prepared by a method analogous to **2a** from 0.090 g (0.28 mmol) of the free carbene and 0.080 g (0.14 mmol) of [Pt(μ-Me$_2$S)Me$_2$]$_2$ in THF. Yield 0.110 g, (72%) of **2b** as a bright yellow air-stable solid. ^{1}H NMR (CD_2Cl_2), δ: 0.19 (3H, s, Pt–C*H*$_3$ *trans* to pyridine, $^2J_{Pt-H}$ = 46.1 Hz), 0.44 (3H, s, Pt–C*H*$_3$ *trans* to carbene, $^2J_{Pt-H}$ = 31.0 Hz), 1.11 (6H, d, $^3J_{H-H}$ = 6.9 Hz, CH(C*H*$_3$)$_2$), 1.37 (6H, d, $^3J_{H-H}$ = 6.9 Hz, CH(C*H*$_3$)$_2$), 2.73 (2H, sept, $^3J_{H-H}$ = 6.9 Hz, C*H*(CH$_3$)$_2$), 2.76 (3H, s, 3-C*H*$_3$-pyridine), 6.90 (1H, d, $^3J_{H-H}$ = 2.2 Hz, ylidene backbone), 7.22 (1H, distorted dd, J_{H-H} = 5.7 Hz, 5.4 Hz and 7.6 Hz, pyridine), 7.35 (2H, d, $^3J_{H-H}$ = 7.9 Hz, aromatic), 7.50 (1H, t, $^3J_{H-H}$ = 7.9 Hz), 7.90 (1H, distorted dd, J_{H-H} = 1.0 Hz, 0.7 Hz and 8.1 Hz, pyridine), 8.04 (1H, d, $^3J_{H-H}$ = 2.2 Hz, ylidene backbone), 9.18 (1H, broad dt, pyridine); ^{13}C{^{1}H} NMR (CD_2Cl_2), δ: −31.2 (s, Pt–CH$_3$, $^1J_{Pt-C}$ = 402.6 Hz), −21.8 (s, Pt–CH$_3$, $^1J_{Pt-C}$ = 397.5 Hz), 19.1 (s, *C*H(CH$_3$)$_2$), 20.3 (s, CH(*C*H$_3$)$_2$), 20.9 (s, CH(*C*H$_3$)$_2$), 23.5 (s, *C*H(CH$_3$)$_2$), 27.5 (s, py-*C*H$_3$), 116.5 (s, ylidene backbone), 120.9 (s, ylidene backbone), 121.6 (s, aromatic), 122.7 (s, aromatic), 122.9 (s, aromatic), 129.0 (s, aromatic), 135.1 (s, aromatic), 141.3 (s, aromatic), 144.2 (s, aromatic), 151.4 (s, aromatic), 189.7 (s, N*C*N, $^1J_{Pt-C}$ = 442.7 Hz); ^{195}Pt{^{1}H}-NMR (D$_2$O), δ:−3763.9. Found: C, 50.12; H, 5.90; N, 7.80%. Calcd for $C_{23}H_{32}N_3Pt$: C, 50.63; H, 5.91; N, 7.70%.

General method for the synthesis of the cationic Pt complexes ***3****,* ***5a–d****,* ***6*** *and* ***8***

Two separate Schlenk tubes were charged with one equiv. of the dimethyl complex and the acid [H(Et$_2$O)$_2$]$^+$[B(Ar^F)$_4$]$^-$, respectively. The two solids were dissolved in CH_2Cl_2, the solutions cooled to −78 °C and the acid solution was added dropwise to the dimethyl complex. Upon addition the colour changed from yellow to almost colourless. The reaction mixture was allowed to warm to −40 °C, when 1.1 equiv. of the dry-degassed pyridine derivative was added by means of a microsyringe, the solution was allowed to reach room temperature slowly and stirred for 30 min. Removal of the volatiles under reduced pressure and washing of the solid residue with petrol gave the pure salt, which was dried under vacuum.

cis-[Pt(κ^2-L1)(CH$_3$)(py)]$^+$[BAr$^F_4$]$^-$ ***3***

This was prepared as above from 0.080 g (0.12 mmol) of complex **1**, 0.113 g (1 equiv.) of acid and 11 μL (1.1 equiv) of pyridine. ^{1}H NMR (CD_2Cl_2), δ: −0.22 (3H, d, Pt–C*H*$_3$, $^3J_{PH}$ = 3.2 Hz, $^2J_{Pt-H}$ = 49.9 Hz), 0.80 (6H, $^3J_{H-H}$ = 6.4 Hz CH(C*H*$_3$)$_2$, species B), 0.93 (6H, $^3J_{H-H}$ = 7.0 Hz CH(C*H*$_3$)$_2$, species A), 1.00 (3H, $^3J_{H-H}$ = 7.0 Hz, CH(C*H*$_3$)$_2$), 1.32 (3H, $^3J_{H-H}$ = 6.4 Hz, CH(C*H*$_3$)$_2$), 2.5 (5H, m, C*H*(CH$_3$)$_2$ and ([PPh$_2$C*H$_2$*CH$_2$-ylidene]PtMe)$^+$ of two species), 2.84 (1H, sept., $^3J_{H-H}$ = 7.0 Hz, C*H*(CH$_3$)$_2$), 4.38 (2H, m, ([PPh$_2$CH$_2$C*H$_2$*-ylidene]PtMe)$^+$), 4.65 (1H, m, ([PPh$_2$CH$_2$C*H$_2$*-ylidene]PtMe)$^+$), 6.89–7.88 (48H, m, aromatics); ^{31}P{^{1}H} (CD_2Cl_2), δ: 8.7 (s, $^1J_{Pt-P}$ = 1977.1 Hz), 10.1 (s, $^1J_{Pt-P}$ = 746.0 Hz); ^{19}F{^{1}H} δ (CD_2Cl_2): −63.1 (s, C*F*$_3$). The reaction was repeated using Et$_2$O as solvent starting from 50 mg (0.075 mmol) of **5.6** and 70 mg (1 equiv.) of acid. Yield after crystallisation: 35 mg, (29%). Anal. Found: C, 50.81; H, 3.42; N, 2.59%. Calcd for $C_{67}H_{53}BF_{24}N_3PPt$: C, 50.52; H, 3.35; N, 2.64%. Colourless needles were obtained by layering an Et$_2$O solution of (**3**) with pentane.

cis-[Pt(κ^2-L1)(CH$_3$)($|^1$-OOCCF$_3$)] ***4*** *(NMR scale experiment)*

Complex **1** (0.020 g, 0.030 mmol) was placed in an NMR tube and dissolved in CD_2Cl_2 resulting in a yellow solution. After the tube was capped with a septum and connected to a nitrogen supply, 3 μL (1.1 equiv.) of CF$_3$COOH were added at room temperature by means of a microsyringe, resulting in the colour changing to almost colourless. The NMR spectra of the solution were recorded. ^{1}H NMR (CD_2Cl_2), δ: 0.08 (3H, d, $^3J_{P-H}$ = 2.9 Hz, $^2J_{Pt-H}$ = 35.5 Hz, Pt–C*H*$_3$), 0.99 (6H, d, $^3J_{H-H}$ = 6.9 Hz, CH(C*H*$_3$)$_2$), 1.12 (6H, d, $^3J_{H-H}$ = 6.9 Hz, CH(C*H*$_3$)$_2$), 2.39 (4H, m, C*H*(CH$_3$)$_2$ and [PPh$_2$C*H$_2$*CH$_2$-ylidene]PtMeO$_2$CCF$_3$), 4.4 (2H, m, [PPh$_2$CH$_2$C*H$_2$*-ylidene]PtMeO$_2$CCF$_3$), 6.88 (1H, d, $^3J_{H-H}$ = 1.9 Hz, ylidene backbone), 7.19 (2H, distorted t, aromatic), 7.22 (6H, broad s, aromatic), 7.33 (1H, d, $^3J_{H-H}$ = 1.8 Hz, ylidene backbone), 7.77 (5H, m, aromatic); ^{31}P{^{1}H} (CD_2Cl_2), δ: 19.6 (s, [*P*Ph$_2$CH$_2$CH$_2$-ylidene]PtMeO$_2$CCF$_3$, $^1J_{Pt-H}$ = 2017.8 Hz); ^{19}F{^{1}H} (CD_2Cl_2), δ: −74.4 (s, [PPh$_2$CH$_2$CH$_2$-ylidene]PtMeO$_2$CC*F*$_3$).

cis-[Pt(κ^2-L2a)(CH$_3$)(py)]$^+$[BAr$^F_4$]$^-$ ***5a***

This was prepared following the general method from 0.049 g (0.09 mmol) of **2a**, 0.085 g (0.09 mmol) acid and 8 μL pyridine in 20 ml CH_2Cl_2. Yield: 0.117 g (88%). ^{1}H NMR (CD_2Cl_2), δ: 0.13 (3H, s, Pt–C*H*$_3$, $^2J_{Pt-H}$ = 40.9 Hz), 1.17 (6H, d, $^3J_{H-H}$ = 6.4 Hz, CH(C*H*$_3$)$_2$), 1.33 (6H, d, $^3J_{H-H}$ = 6.4 Hz, CH(C*H*$_3$)$_2$), 2.61 (2H, $^3J_{H-H}$ = 6.4 Hz, C*H*(CH$_3$)$_2$), 6.98 (1H, d, $^3J_{H-H}$ = 1.5 Hz, imidazol-2-ylidene backbone), 7.23 (2H, distorted ddd, J_{H-H} = 5.7 Hz, 5.4 Hz and 7.6 Hz, pyridine), 7.33 (2H, d, $^3J_{H-H}$ = 7.9 Hz, aromatic), 7.49 (1H, t, $^3J_{H-H}$ = 7.9 Hz, aromatic), 7.90 (1H, distorted ddd, J_{H-H} = 1 Hz,

0.7 Hz and 8.2 Hz, pyridine), 8.06 (1H, d, $^3J_{H-H}$ = 1.5 Hz, imidazol-2-ylidene backbone), 9.19 (broad dt, 1H, pyridine); $^{13}C\{^1H\}$ NMR (CD_2Cl_2), δ: −16.8 (s, $^1J_{Pt-C}$ = 517.7 Hz, Pt−CH_3), 19.1 (s, CH(CH_3)$_2$), 19.9 (s, CH(CH_3)$_2$), 23.5 (s, CH(CH_3)$_2$), 117.1 (s, imidazol-2-ylidene backbone), 118.1 (imidazol-2-ylidene backbone), 120.1 (s, aromatic), 121.1 (s, aromatic), 122.5 (s, aromatic), 123.3 (s, aromatic), 123.8 (s, aromatic), 125.0 (s, aromatic), 125.4 (s, aromatic), 126.3 (s, aromatic), 128.2 (q, $^2J_{F-C}$ = 28.3 Hz, aromatic), 130.3 (s, aromatic), 134.0 (s, aromatic), 138.7 (s, aromatic), 143.3 (s, aromatic), 144.1 (s, aromatic), 144.3 (s, aromatic), 150.4 (s, aromatic), 160.9 (q, $^1J_{F-C}$ = 43.8 Hz, CF_3); $^{19}F\{^1H\}$,(CD_2Cl_2), δ: −63.1 (s, CF_3); $^{195}Pt\{^1H\}$ NMR (CD_2Cl_2): −3495.8. Found: C, 47.25; H, 3.00; N, 3.70%. Calcd for $C_{58}H_{44}BF_{24}N_4Pt$: C, 47.75; H, 3.04; N, 3.84%.

cis-[Pt(κ²-L2b)(CH$_3$)(py)]$^+$[BAr$^F_4$]$^-$ ***5b***

This salt was prepared following the general method from 0.050 g (0.09 mmol) of **2b**, 0.085 g (0.09 mmol) acid and 8 μL pyridine in 20 ml CH_2Cl_2. Yield: 0.118 g, (89%). ^1H NMR (CD_2Cl_2), δ: 0.14 (3H, s, Pt−CH_3, $^2J_{Pt-H}$ = 40.2 Hz), 1.15 [6H, d, $^3J_{H-H}$ = 6.4 Hz, CH(CH_3)$_2$], 1.33 [6H, d, $^3J_{H-H}$ = 6.4 Hz, CH(CH_3)$_2$], 2.65 [2H, sept., $^3J_{H-H}$ = 6.4 Hz, CH(CH_3)$_2$], 2.81 (3H, s, 3-CH_3-pyridine), 7.05 (1H, m, imidazol-2-ylidene backbone), 7.21 (1H, m, aromatic), 7.33 (2H, distorted d., aromatic), 7.53 (6H, broad s., aromatic), 7.74 (10H, broad s., aromatic), 7.92 (2H, m, aromatic), 8.10 (1H, d, J_{H-H} = 2.7 Hz, aromatic), 8.52 (2H, m, aromatic); $^{13}C\{^1H\}$ NMR (CD_2Cl_2), δ: −16.5 (s, Pt−CH_3, $^1J_{Pt-C}$ = 519.9 Hz), 19.8 [s, CH(CH_3)$_2$], 22.2 [s, CH(CH_3)$_2$], 23.6 [s, CH(CH_3)$_2$], 27.8 (s, py-CH_3), 116.7 (s, ylidene backbone), 118.1 (imidazol-2-ylidene backbone), 119.8 (s, aromatic), 122.5 (s, aromatic), 123.2 (s, aromatic), 123.6 (s, aromatic), 125.0 (s, aromatic), 125.2 (s, aromatic), 126.3 (s, aromatic), 128.1 (q, $^2J_{F-C}$ = 28.8 Hz, aromatic), 130.2 (s, aromatic), 134.0 (s, aromatic), 138.4 (s, aromatic), 143.3 (s, aromatic), 144.1 (s, aromatic), 144.3 (s, aromatic), 150.4 (s, aromatic), 160.9 (q, $^1J_{F-C}$ = 43.9 Hz, CF_3); $^{19}F\{^1H\}$} NMR (CD_2Cl_2), δ: −63.1 (s, CF_3); ^{195}Pt $\{^1H\}$ NMR (CD_2Cl_2), δ: −3496.4. Colourless crystals suitable for single crystal X-ray diffraction were grown by slow diffusion of petrol into an ether solution of **9b**. Found: C, 47.82; H, 3.10; N, 3.72%. Calcd for $C_{59}H_{46}BF_{24}N_4Pt$: C, 48.11; H, 3.15; N, 3.80%.

cis-[Pt(κ²-L2a)(CH$_3$)(2-fluoro-pyridine)]$^+$[BAr$^F_4$]$^-$ ***5c***

This was prepared following the general method from 0.050 g (0.09 mmol) of **2a**, 0.088 g (1 equiv.) of acid and 6 L (1.1 equiv.) of 2-fluoro-pyridine. Yield: 0.105 g (77%). ^1H NMR (CD_2Cl_2), δ: 0.11 (3H, s, Pt−CH_3, $^2J_{Pt-H}$ = 39.5 Hz), 1.17 [6H, d, $^3J_{H-H}$ = 7.3 Hz, CH(CH_3)$_2$], 1.25 (6H, d, $^3J_{H-H}$ = 7.3 Hz, CH(CH_3)$_2$), 2.67 [2H, sept., $^3J_{H-H}$ = 7.3 Hz, CH(CH_3)$_2$], 7.03 (1H, d, $^3J_{H-H}$ = 2.2 Hz, imidazol-2-ylidene backbone), 7.30 (3H, q, $^3J_{H-H}$ = 7.3 Hz, aromatic), 7.42 (1H, t, $^3J_{H-H}$ = 6.6 Hz, aromatic), 7.55 (5H, broad s, aromatic), 7.68 (1H, d, J_{H-H} = 8.0 Hz, aromatic), 7.84 (11H, broad s., aromatic), 7.89 (1H, d, $^3J_{H-H}$ = 2.2 Hz, imidazol-2-ylidene backbone), 8.16 (1H, dt, J_{H-H} = 1.5 Hz, 8.0 Hz, aromatic), 8.32 (2H, m, aromatic); $^{13}C\{^1H\}$-NMR (CD_2Cl_2), δ: −3.2 (s, Pt−CH_3, $^1J_{Pt-C}$ = 542.8 Hz), 18.4 [s, CH(CH_3)$_2$], 23.6 [s, CH(CH_3)$_2$], 27.9 [s, CH(CH_3)$_2$], 116.7 (s, imidazol-2-ylidene backbone), 117.3 (s, imidazol-2-ylidene backbone), 119.7 (s, aromatic), 122.5 (s, imidazol-2-ylidene backbone), 122.9 (s, aromatic), 123.7 (s, aromatic), 125.2 (s, aromatic), 125.9 (s, aromatic), 128.0 (q, $^2J_{F-C}$ = 28.5 Hz, aromatic), 130.4 (s, aromatic), 132.1 (s, aromatic), 134.0 (s, aromatic), 136.2 (d, $^2J_{F-C}$ = 18.3 Hz, 2-F-pyridine), 140.3 (d, $^1J_{F-C}$ = 33.1 Hz, 2-F-pyridine carbon), 141.1 (s, aromatic), 145.6 (s, aromatic), 148.3 (s, aromatic), 160.7 (q, $^1J_{F-C}$ = 43.6 Hz, CF_3 s); $^{19}F\{^1H\}$ NMR (CD_2Cl_2): −63.1 (s, CF_3 s), -61.1 (s, 2-F-pyridine). Colourless crystals were grown by layering an ether solution of **5c** with pentane. Found: C, 46.87; H, 2.80; N, 3.67%. Calcd. for $C_{58}H_{43}BF_{25}N_4Pt$: C, 47.17; H, 2.93; N, 3.79%.

cis-[Pt(κ²-L2a)(CH$_3$)(2,6-difluoro-pyridine)]$^+$[BAr$^F_4$]$^-$ ***5d***

This was prepared following the general method from 0.050 g (0.09 mmol) of complex **2a**, 0.088 g (1 equiv.) of acid$^-$ and 6 μL (1.3 equiv.) of 2,6-difluoro-pyridine. Yield: 0.105 g (76%). ^1H NMR (CD_2Cl_2), δ: 0.13 (3H, s, Pt−CH_3, $^2J_{Pt-H}$ = 38.4 Hz), 1.11 (6H, d, $^3J_{H-H}$ = 6.9 Hz, CH(CH_3)$_2$), 1.30 (6H, d, $^3J_{H-H}$ = 6.9 Hz, CH(CH_3)$_2$), 2.65 (2H, sept., $^3J_{H-H}$ = 6.9 Hz, CH(CH_3)$_2$), 7.08 (1H, d, $^3J_{H-H}$ = 2.2 Hz, imidazol-2-ylidene backbone), 7.21 (1H, d $^3J_{H-H}$ = 8.2 Hz, aromatic), 7.33 (3H, m, aromatic), 7.53 (4H, broad s., aromatic), 7.63 (1H, d, $^3J_{H-H}$ = 8.5 Hz, aromatic), 7.70 (8H, broad s, aromatic), 7.77 (3H, m, aromatic), 8.19 (2H, m, aromatic); $^{13}C\{^1H\}$ NMR, (CD_2Cl_2), δ: −2.6 (s, Pt−CH_3, $^1J_{Pt-C}$ = 518.1 Hz), 19.8 (s, CH(CH_3)$_2$), 22.6 (s, CH(CH_3)$_2$), 24.1 (s, CH(CH_3)$_2$), 116.9 (s, imidazol-2-ylidene backbone), 117.9 (imidazol-2-ylidene backbone), 119.8 (s, aromatic), 122.5 (s, aromatic), 123.2 (s, aromatic), 123.6 (s, aromatic), 125.0 (s, aromatic), 125.2 (s, aromatic), 126.3 (s, aromatic), 128.1 (q, $^2J_{F-C}$ = 28.8 Hz, aromatic), 130.2 (s, aromatic), 134.0 (s, aromatic), 138.4 (d, $^2J_{F-C}$ = 19.0 Hz, 2, 6-F_2-pyridine), 143.3 (s, aromatic), 144.1 (d, $^1J_{F-C}$ = 32.9 Hz, 2, 6-F_2-pyridine carbon), 144.3 (s, aromatic), 150.4 (s, aromatic), 160.9 (q, $^1J_{F-C}$ = 43.9 Hz, CF_3); ^{19}F $\{^1H\}$} NMR (CD_2Cl_2), δ: −63.1 (s, CF_3), −60.3 (s, 2, 6-F_2-pyridine, J_{Pt-F} = 110.1 Hz). Colourless crystals were grown by layering an ether solution of **5d** with pentane. Found: C, 46.32; H, 2.65; N, 3.61%. Calcd. for $C_{58}H_{42}BF_{26}N_4Pt$: C, 46.60; H, 2.83; N, 3.75%.

cis-[Pt(κ²-L2a)(CH$_3$)(Et$_2$O)]$^+$[BAr$^F_4$]$^-$ ***6***

This was prepared following the general method from 0.050 g (0.09 mmol) of **2a**, 0.088 g (1 equiv.) of acid$^-$ and 5 μL of trifluoroethanol (1 equiv.). Since the primary products from the reaction could not be characterised, the volatiles were removed under reduced pressure and the solid residue was dissolved in ether and was layered with petrol to give colourless crystals of **6**. Yield: 0.025 g (19%). ^1H NMR (d_5-PhCl), δ: 0.22 (s, Pt−CH_3, $^2J_{Pt-H}$ = 35.1 Hz), 1.13 (6H, d, $^3J_{H-H}$ = 6.9 Hz, CH(CH_3)$_2$), 1.21 (12H, m, coordinated and uncoordinated (CH_3CH_2)$_2$O), 1.32 (6H, d, $^3J_{H-H}$ = 6.9 Hz, CH(CH_3)$_2$), 2.59 (2H, d, $^3J_{H-H}$ = 6.9 Hz, CH(CH_3)$_2$), 3.40 (4H, q, $^3J_{H-H}$ = 6.9 Hz, uncoordinated (CH_3CH_2)$_2$O), 3.53 (4H, broad q, $^3J_{H-H}$ = 7.1 Hz, coordinated (CH_3CH_2)$_2$O), 6.70 Hz (1H, d, $^3J_{H-H}$ = 2.2 Hz, imidazol-2-ylidene backbone), 6.78 (1H, d, $^3J_{H-H}$ = 8.5 Hz, aromatic), 7.09 (6H, m, aromatic), 7.23 (7H, m, aromatic), 7.48 (4H, m, aromatic), 8.23 (1H, m, aromatic), 8.46 (1H, m, aromatic); $^{19}F\{^1H\}$-NMR (d_5-PhCl), δ: −63.6 (s, CF_3 s); $^{195}Pt\{^1H\}$ NMR (d_5-PhCl), δ: −3703. Satisfactory analytical data for **6** could not be obtained presumably due to the facile loss of coordinated ether.

cis-[Pt(κ²-L2a)(CH$_3$)[(C$_6$F$_5$)$_3$B(OH)] ***8***

In a solution of 0.060 g (0.12 mmol) of **2a** and 0.061 g (1 equiv.) of B(C_6F_5)$_3$ in ether (15 ml) was added H_2O (two drops) at room temperature and the solution was immediately cooled to −78 °C. The mixture was allowed to warm slowly to room temperature and stirred overnight. After removal of the volatiles under reduced pressure the resulting off-white solid was dried under vacuum, washed with petrol and dried under vacuum. Yield: 0.050 g (40%). ^1H NMR (CD_2Cl_2) δ: −0.01 (3H, s, Pt−CH_3 $^2J_{Pt-H}$ = 37.7 Hz), 1.06 (6H, d, $^3J_{H-H}$ = 6.8 Hz, CH(CH_3)$_2$), 1.15 (6H, d, $^3J_{H-H}$ = 6.8 Hz, CH(CH_3)$_2$), 2.49 (2H, sept., $^3J_{H-H}$ = 6.8 Hz, CH(CH_3)$_2$), 2.93 (1H, broad s., OH(B(C_6F_5)$_3$), 6.89 (1H, $^3J_{H-H}$ = 2.4 Hz, imidazol-2-ylidene backbone), 7.21 (2H, $^3J_{H-H}$ = 7.9 Hz, aromatic), 7.45 (3H, m, aromatic), 7.53 (1H, d, $^3J_{H-H}$ = 2.4 Hz, imidazol-2-ylidene backbone), 8.12 (1H, dt, J_{H-H} = 1.7 Hz, 8.1 Hz, aromatic), 8.56 (1H, broad d., $^3J_{H-H}$ = 5.5 Hz, aromatic); $^{19}F\{^1H\}$ NMR (CD_2Cl_2), δ: −165.9 (d, $^2J_{F-F}$ = 19.3 Hz, *o*-F of B(C_6F_5)$_3$), −161.0 (t, $^2J_{F-F}$ = 19.3 Hz, *m*-F of B(C_6F_5)$_3$), −134.5 (m, *p*-F of B(C_6F_5)$_3$); I.R. (Nujol, cm^{-1}): 3599 (s, OH stretching). Colourless crystals of compound **8** were grown by slow diffusion of

pentane into an ether solution. Found: C, 45.15; H, 2.93; N, 3.42%. Calcd for $C_{45}H_{36}BF_{18}N_3OPt$: C, 45.70; H, 3.07; N, 3.55%.

Formation of cis-[Pt(κ^2-L2a)(CH_3)(μ^1-OOCCF$_3$) ***9*** *(NMR scale experiment)*

Complex **2a** (0.015 g, 0.03 mmol) was placed in an NMR tube and dissolved in CD_2Cl_2 resulting in a bright yellow solution. After the tube was capped with a septum and connected to a nitrogen supply, 3 μL (1.1 equiv.) of CF_3COOH were added at room temperature by means of a microsyringe, resulting in the colour changing to almost colourless. The NMR spectra of the solution were recorded. ^{1}H NMR (CD_2Cl_2), δ: 0.17 (3H, s, Pt–C*H*$_3$, $^2J_{Pt-H}$ = 38.6 Hz), 1.12 (6H, d, $^3J_{H-H}$ = 6.8 Hz, CH(C*H*$_3$)$_2$), 1.29 (6H, d, $^3J_{H-H}$ = 6.8 Hz, CH(C*H*$_3$)$_2$), 2.50 (2H, sept., $^3J_{H-H}$ = 6.8 Hz, C*H*(CH$_3$)$_2$), 6.94 (1H, d, $^3J_{H-H}$ = 2.3 Hz, imidazol-2-ylidene backbone), 7.29 (2H, d, $^3J_{H-H}$ = 7.8 Hz, aromatic), 7.51 (3H, m, aromatic), 7.66 (1H, d, $^3J_{H-H}$ = 2.3 Hz, imidazol-2-ylidene backbone), 8.14 (1H, ddd, J_{H-H} = 1.6 Hz, 7.5 Hz, 9.8 Hz, aromatic), 8.59 (1H, ddd, J_{H-H} = 0.9 Hz, 1.6 Hz, 4.6 Hz, aromatic); ^{13}C{^{1}H} NMR (CD_2Cl_2), δ: −19.7 (s, Pt–CH$_3$, $^1J_{Pt-C}$ = 266.3 Hz), 23.5 (s, CH(*C*H$_3$)$_2$), 25.0 (s, CH(*C*H$_3$)$_2$), 29.1 (s, *C*H(CH$_3$)$_2$), 110.8 (s, imidazol-2-ylidene backbone), 115.6 (s, imidazol-2-ylidene backbone), 124.2 (s, aromatic), 124.7 (s, aromatic), 126.3 (s, aromatic), 131.2 (s, aromatic), 135.3 (s, aromatic), 141.0 (s, aromatic), 145.9 (s, aromatic), 147.6 (s, aromatic), 150.8 (s, aromatic); ^{19}F{^{1}H} δ(CD_2Cl_2): −75.4 (s, C*F*$_3$COO$^-$).

Reaction of ***1a*** *with MeI. Formation of* ***10*** *(NMR scale experiment)*

Complex **1a** (20 mg (0.030 mmol) was dissolved in CD_2Cl_2 in a Youngs' NMR tube. To the solution at room temperature were added 4 μL of MeI and the NMR spectra were recorded. ^{1}H NMR (CD_2Cl_2), δ: 0.23 (3H, d, $^3J_{P-H}$ = 8.2 Hz, $^2J_{Pt-H}$ = 36.3 Hz, Pt–C*H*$_3$), 0.74, 0.83, 0.98, 1.10, 1.25, 1.39 (18H, overlapping each d, remaining Pt–C*H*$_3$ and CH(C*H*$_3$)$_2$), 2.38 (1H, sept., $^3J_{H-H}$ = 6.8 Hz, C*H*(CH$_3$)$_2$), 2.53 (1H, m, (PPh$_2$C*H*$_2$CH$_2$-ylidene)PtMe$_3$I), 2.78 (1H, sept., $^3J_{H-H}$ = 6.9 Hz, C*H*(CH$_3$)$_2$), 2.95 (1H, m, [PPh$_2$C*H*$_2$CH$_2$-ylidene]PtMe$_3$I), 4.31 (1H, m, (PPh$_2$CH$_2$C*H*$_2$-ylidene)PtMe$_3$I), 5.64 (1H, m, (PPh$_2$CH$_2$C*H*$_2$-ylidene)PtMe$_3$I), 6.79 (1H, broad s, imidazol-2-ylidene backbone), 7.15 (4H, m, aromatic), 7.33 (3H, broad s, aromatic), 7.42 (5H, broad m, aromatic and backbone imidazol-2-ylidene), 8.11 (2H, m, aromatic); ^{31}P{^{1}H} NMR: δ, (CD_2Cl_2): 10.8 (s, [*P*Ph$_2$CH$_2$CH$_2$-ylidene]PtMe$_3$I, $^1J_{Pt-P}$ = 799.6 Hz).

Reaction of ***2a*** *with MeI. Formation of* ***11***

Complex **2a** (0.055 g (0.10 mmol) was dissolved in 15 ml of CH_2Cl_2 and 9 L (1.1 equiv.) of MeI was added *via* a microsyringe. The mixture was stirred at room temperature for 30 min upon which time the colour changed from bright to pale yellow. After removal of the volatiles under reduced pressure, the resulting pale yellow solid was washed with petrol (2 × 10 ml) to yield 0.062 g (89%) of **11**. ^{1}H NMR, (CD_2Cl_2), δ: 0.32–1.12 (6H, three singlets with Pt satellites, $^2J_{Pt-H}$ = 38.1 Hz, 38.1 Hz and 26.4 Hz, Pt(CN)Me$_3$I), 1.22 (6H, apparent t, CH(C*H*$_3$)$_2$), 1.25 (3H, d, $^3J_{H-H}$ = 7.3 Hz, CH(C*H*$_3$)$_2$), 1.30 (3H, d, $^3J_{H-H}$ = 7.3 Hz, CH(C*H*$_3$)$_2$), 2.55 (sept., 1H, $^3J_{H-H}$ = 7.3 Hz, C*H*(CH$_3$)$_2$), 3.41 (sept., 1H, $^3J_{H-H}$ = 7.3 Hz, C*H*(CH$_3$)$_2$), 6.93 (s, 1H, imidazol-2-ylidene backbone), 7.22 (1H, d, aromatic, $^3J_{H-H}$ = 7.3 Hz), 7.28 (1H, d, $^3J_{H-H}$ = 7.3 Hz, aromatic), 7.38 (1H, t, $^3J_{H-H}$ = 7.3 Hz, aromatic), 7.41 (1H, t, $^3J_{H-H}$ = 8.8 Hz, py-H4), 7.59 (1H, d, $^3J_{H-H}$ = 8.8 Hz, py-H3), 7.77 (1H, s, imidazol-2-ylidene backbone), 8.05 (1H, t, $^3J_{H-H}$ = 8.8 Hz, py-H5), 8.61 (1H, d, $^3J_{H-H}$ = 8.8 Hz, py-H6); ^{13}C{^{1}H} NMR (CD_2Cl_2), δ: −32.8 (s, with one Pt satellite, $^1J_{Pt-C}$ = 328.5 Hz, Pt(CN)*Me*$_3$I), −20.5 (s, $^1J_{Pt-C}$ = 146.8 Hz, Pt(CN)*Me*$_3$I), −10.6 [s, $^1J_{Pt-C}$ = 330.4 Hz, Pt(CN)*Me*$_3$I], 20.7, 21.8, 24.1, 24.3, 26.5, 26.6 (s, CH(*C*H$_3$)$_2$)), 110.2 (s, aromatic), 114.2 (s, aromatic), 121.4 (s, aromatic), 121.8 (s, aromatic), 122.6 (s, aromatic), 124.8 (s, aromatic), 128.8 (s, aromatic), 132.3 (s, aromatic), 138.9 (s, aromatic), 143.9 (s, aromatic), 145.1 (s, aromatic), 145.2 (s, aromatic), 149.8 (s, aromatic), 183.4 (s, NCN, $^1J_{Pt-C}$ = 421.8 Hz). Yellow, X-ray quality crystals were obtained by layering a CH_2Cl_2 solution with light petroleum (40–60). Found: C, 40.85; H, 4.78; N, 6.10%.Calcd. for $C_{23}H_{33}IN_3Pt$: C, 41.02; H, 4.94; N, 6.24%.

X-ray crystallography

A summary of the crystal data, data collection and refinement data for complexes **1**, **2a**, **2b**Cl, **5b**, **5c**, **6**, **8**, and **11** are given in Table 1. Data sets were collected on an Enraf-Nonius Kappa CCD

Table 1
Summary of crystal data collection and refinement data for complexes **1**, **2a**, **2b**Cl, **5b**, **5c**, **6**, **8**, and **11**.

Complex	**1**	**2a**	**2b**Cl	**5b**	**5c**	**6**	**8**·ether	**11**
CCDC	986051	986052	986053	986054	986055	986056	986057	986058
Formula	$C_{31}H_{39}N_2PPt$	$C_{22}H_{29}N_3Pt$	$C_{22}H_{28}ClN_3Pt$	$C_{59}H_{45}BF_{24}N_4Pt$	$C_{58}H_{42}BF_{25}N_4Pt$	$C_{57}H_{48}BF_{24}N_3OPt$	$C_{43}H_{37}BF_{15}N_3O_2Pt$	$C_{23}H_{32}N_3Pt$
Formula weight	665.7	530.57	565.01	1471.89	1475.86	1452.88	1118.66	672.51
λ (Å)	0.71073	0.71073	0.71073	0.71073	0.71073	0.71073	0.71073	0.71073
Crystal system	Monoclinic	Monoclinic	Monoclinic	Triclinic	Triclinic	Triclinic	Triclinic	Monoclinic
Space group	P21/n	P21/n	P21/n	P -1	P-1	P-1	P-1	P21/n
a (Å)	12.5675(19)	8.7905(7)	9.0112(8)	13.4405(7)	14.1039(11)	14.285(2)	10.734(6)	8.5894(6)
b (Å)	15.1164(10)	18.482(2)	17.2104(16)	15.1552(6)	15.1745(8)	14.324(1)	11.247(8)	29.989(4)
c (Å)	15.212(3)	12.4068(10)	13.1379(12)	15.487(1)	15.231(1)	15.645(1)	19.611(16)	9.633(1)
α (°)	90	90	90	76.778(5)	92.894(6)	97.346(7)	81.61(7)	90
β (°)	110.368(14)	98.768(7)	93.787(2)	84.170(5)	96.530(6)	96.952(9)	79.13(5)	103.39(1)
γ (°)	90	90	90	72.930(4)	99.627(4)	97.259(9)	71.43(4)	90
Volume (Å^3)	2709.3(7)	1992.1(3)	2033.1(3)	2934.0(3)	3184.9(4)	3118.5(5)	2195(3)	2413.9(5)
Z	4	4	4	2	2	2	2	4
μ (mm^{-1})	5.26	7.054	7.045	2.51	2.319	2.36	3.301	7.104
Reflections	32044	39241	24137	41301	58202	61790	29558	23820
Indepen. reflections (*R*(int))	6307 (0.0576)	4620 (0.0587)	4669 (0.0534)	13520 (0.0590)	14459 (0.1395)	14423 (0.0554)	7699 (0.1070)	5495 (0.0536)
GoF	1.004	1.039	1.043	1.023	1	0.894	1.05	1.04
Final *R* ($I > 2\sigma(I)$) *R*1 (*wR*(F^2))	0.0317 (0.0613)	0.0362 (0.0654)	0.0421 (0.0573)	0.0368 (0.0837)	0.0673 (0.1495)	0.0534 (0.1250)	0.0842 (0.2244)	0.0320 (0.0607)
Final R (all data) *R*1 (*wR*(F^2))	0.0539 (0.0667)	0.0618 (0.0735)	0.0904 (0.0969)	0.0438 (0.0871)	0.1238 (0.1680)	0.0728 (0.1358)	0.1144 (0.2453)	0.0502 (0.0665)

area detector diffractometer with an FR591 rotating anode (Mo-Kα radiation) and an Oxford Cryosystems low temperature device, operating in ω scanning mode with ψ and ω scans to fill the Ewald sphere. The software used for control and integration were Collect, Scalepack, and Denzo [39]. The structures were solved by direct methods using the program SHELXS-97 [40]. The refinement and all further calculations were carried out using SHELXL-97 [41]. The H-atoms were included in calculated positions and treated as riding atoms using SHELXL default parameters. The non-H atoms were refined anisotropically, using weighted full-matrix least-squares on F^2.

In the structure of **5c** the anion contains F atoms of one CF_3 group that are severely disordered and were modelled by restraining their thermal parameters. Furthermore, the coordinated 2-fluoropyridine was also disordered in two positions that were successfully modelled using standard Shelxl methodology; finally the structure contains one molecule of disordered solvent molecule (corresponding to ether) which could not be modelled satisfactorily. A Platon SQUEEZE algorithm [42] was applied to remove the residual electron density. The crystals used for the determination of the structure of **6** were of pure quality giving weak reflections at wide angles; as a result the data set was not complete. Furthermore, the structure contains one molecule of disordered solvent molecule (ether see also discussion of the NMR spectra above) which could not be modelled satisfactorily and the residual electron density was removed by applying the Platon SQUEEZE algorithm.

Acknowledgements

A.A.D. thanks the USIAS, the CNRS and the Région Alsace, Communauté Urbaine de Strasbourg for the award of fellowships and a Gutenberg Excellence Chair (2010-11), respectively.

Appendix A. Supplementary material

CCDC 986051, 986052, 986053, 986054, 986055, 986056, 986057 and 986058 contain the supplementary crystallographic data for this paper. These data can be obtained free of charge from The Cambridge Crystallographic Data Centre via www.ccdc.cam.ac.uk/data_request/cif.

References

[1] A.J. Arduengo, S.F. Gamper, J.C. Calabrese, F. Davidson, J. Am. Chem. Soc. 116 (1994) 4391–4394.
[2] A. Danopoulos, *N*-Heterocyclic carbene complexes in additions to multiple bonds, in: C.S.J. Cazin (Ed.), *N*-Heterocyclic Carbenes in Transition Metal Catalysis and Organocatalysis, Springer, Netherlands, 2011, pp. 23–61.
[3] G. De Bo, G. Berthon-Gelloz, B. Tinant, I.E. Markó, Organometallics 25 (2006) 1881–1890.
[4] M.A. Duin, N.D. Clement, K.J. Cavell, C.J. Elsevier, Chem. Commun. (2003) 400–401.
[5] G.C. Fortman, N.M. Scott, A. Linden, E.D. Stevens, R. Dorta, S.P. Nolan, Chem. Commun. 46 (2010) 1050–1052.
[6] O. Rivada-Wheelaghan, M.A. Ortuno, S.E. Garcia-Garrido, J. Diez, P.J. Alonso, A. Lledos, S. Conejero, Chem. Commun. 50 (2014) 1299–1301.
[7] R. Lindner, C. Wagner, D. Steinborn, J. Am. Chem. Soc. 131 (2009) 8861–8874.
[8] A.E. Shilov, G.B. Shul'pin, Activation and Catalytic Reactions of Saturated Hydrocarbons in the Presence of Metal Complexes, Kluwer, 2000.
[9] D. Meyer, S. Ahrens, T. Strassner, Organometallics 29 (2010) 3392–3396.
[10] Y. Unger, A. Zeller, M.A. Taige, T. Strassner, Dalton Trans. (2009) 4786–4794.
[11] A. Huffer, B. Jeffery, B.J. Waller, A.A. Danopoulos, C. R. Chim. 16 (2013) 557–565.
[12] D. Serra, P. Cao, J. Cabrera, R. Padilla, F. Rominger, M. Limbach, Organometallics 30 (2011) 1885–1895.
[13] P. Cao, J. Cabrera, R. Padilla, D. Serra, F. Rominger, M. Limbach, Organometallics 31 (2012) 921–929.
[14] C.-S. Lee, R.R. Zhuang, S. Sabiah, J.-C. Wang, W.-S. Hwang, I.J.B. Lin, Organometallics 30 (2011) 3897–3900.
[15] K. Li, Y. Chen, W. Lu, N. Zhu, C.-M. Che, Chem. Eur. J. 17 (2011) 4109–4112.
[16] R. Wai-Yin Sun, A. Lok-Fung Chow, X.-H. Li, J.J. Yan, S. Sin-Yin Chui, C.-M. Che, Chem. Sci. 2 (2011) 728–736.
[17] E.M. Prokopchuk, R.J. Puddephatt, Organometallics 22 (2002) 563–566.
[18] N. Tsoureas, A.A. Danopoulos, A.A.D. Tulloch, M.E. Light, Organometallics 22 (2003) 4750–4758.
[19] A.A. Danopoulos, N. Tsoureas, S.A. Macgregor, C. Smith, Organometallics 26 (2006) 253–263.
[20] J.A. Osborn, R.R. Schrock, J. Am. Chem. Soc. 93 (1971) 3089–3091.
[21] R. Crabtree, Acc. Chem. Res. 12 (1979) 331–337.
[22] S.D. Ittel, L.K. Johnson, M. Brookhart, Chem. Rev. 100 (2000) 1169–1204.
[23] M. Lersch, M. Tilset, Chem. Rev. 105 (2005) 2471–2526.
[24] C. Tsay, N.P. Mankad, J.C. Peters, J. Am. Chem. Soc. 132 (2010) 13975–13977.
[25] A. Abo-Amer, M.S. McCready, F. Zhang, R.J. Puddephatt, Can. J. Chem. 90 (2011) 46–54.
[26] M.W. Holtcamp, L.M. Henling, M.W. Day, J.A. Labinger, J.E. Bercaw, Inorg. Chim. Acta 270 (1998) 467–478.
[27] S.J. Mitton, R. McDonald, L. Turculet, Organometallics 28 (2009) 5122–5136.
[28] E. Szuromi, P.R. Sharp, Organometallics 25 (2005) 558–559.
[29] J.C. Thomas, J.C. Peters, J. Am. Chem. Soc. 125 (2003) 8870–8888.
[30] W.V. Konze, B.L. Scott, G.J. Kubas, J. Am. Chem. Soc. 124 (2002) 12550–12556.
[31] A.A. Danopoulos, J.R. Galsworthy, M.L.H. Green, L.H. Doerrer, S. Cafferkey, M.B. Hursthouse, Chem. Commun. (1998) 2529–2560.
[32] G.S. Hill, L. Manojlovic-Muir, K.W. Muir, R.J. Puddephatt, Organometallics 16 (1997) 525–530.
[33] G.S. Hill, G.P.A. Yap, R.J. Puddephatt, Organometallics 18 (1999) 1408–1418.
[34] D.M. Crumpton-Bregel, K.I. Goldberg, J. Am. Chem. Soc. 125 (2003) 9442–9456.
[35] G.S. Hill, M.J. Irwin, C.J. Levy, L.M. Rendina, R.J. Puddephatt, R.A. Andersen, L. McLean, Inorg. Synth. (1998) 149–153. John Wiley & Sons, Inc.
[36] A.A.D. Tulloch, A.A. Danopoulos, S. Winston, S. Kleinhenz, G. Eastham, J. Chem. Soc. Dalton Trans. (2000) 4499–4506.
[37] A.A. Danopoulos, S. Winston, T. Gelbrich, M.B. Hursthouse, R.P. Tooze, Chem. Commun. (2002) 482–483.
[38] M. Brookhart, B. Grant, A.F. Volpe, Organometallics 11 (1992) 3920–3922.
[39] Z. Otwinowski, W. Minor, Processing of X-ray diffraction data collected in oscillation mode, in: Charles W. Carter Jr. (Ed.), Methods Enzymol., Academic Press, 1997, pp. 307–326.
[40] G.M. Sheldrick, SHELXL, University of Göttingen, Göttingen, 1999.
[41] G.M. Sheldrick, Acta Crystallogr. Sect. A 46 (1990) 467–473.
[42] A. Spek, J. Appl. Crystallogr. 36 (2003) 7–13.